Spontaneous Transition of Turbulent Flames to Detonations in Unconfined Media

Alexei Y. Poludnenko,[1,*] Thomas A. Gardiner,[2] and Elaine S. Oran[1]
[1]*Naval Research Laboratory, Washington, D.C. 20375, USA*
[2]*Sandia National Laboratories, Albuquerque, New Mexico 87185-1189, USA*
(Received 29 March 2011; published 27 July 2011)

A deflagration-to-detonation transition (DDT) can occur in environments ranging from experimental and industrial systems to astrophysical thermonuclear (type Ia) supernovae explosions. Substantial progress has been made in explaining the nature of DDT in confined systems with walls, internal obstacles, or preexisting shocks. It remains unclear, however, whether DDT can occur in unconfined media. Here we use direct numerical simulations (DNS) to show that for high enough turbulent intensities unconfined, subsonic, premixed, turbulent flames are inherently unstable to DDT. The associated mechanism, based on the nonsteady evolution of flames faster than the Chapman-Jouguet deflagrations, is qualitatively different from the traditionally suggested spontaneous reaction-wave model. Critical turbulent flame speeds, predicted by this mechanism for the onset of DDT, are in agreement with DNS results.

DOI: 10.1103/PhysRevLett.107.054501 PACS numbers: 47.70.Pq, 47.40.Rs, 97.60.Bw

Since the discovery of detonations, the question of the physical mechanisms that create these self-supporting, supersonic, shock-driven reaction waves has been a forefront topic in combustion theory. Uncontrolled development of detonations poses significant threats to chemical storage and processing facilities, mining operations, etc. [1], while controlled detonation initiation in propulsion systems could revolutionize transportation [2]. On astrophysical scales, detonation formation is presently the most important, yet least understood, aspect of the explosion [3,4] powering type Ia supernovae, which, as standard cosmological distance indicators, led to the discovery of the accelerating expansion of the Universe [5,6].

Early studies [7] showed that a detonation can arise from a slow, highly subsonic deflagration ignited in an initially unpressurized system. Significant progress has since been made experimentally [8] and numerically [9–12] in elucidating the physics of the deflagration-to-detonation transition (DDT) in confined systems, and particularly in closed channels. These studies showed that the confining effect of channel walls on the hot, expanding products of burning and the interaction of the resulting flow with walls and obstacles are important in accelerating the flame and causing the pressure increase, thus creating conditions necessary for the detonation ignition. This raises the question: Is DDT possible in unconfined media without assistance of walls or obstacles, e.g., in unconfined clouds of fuel vapor or in the interior of a white dwarf star during a supernova explosion?

Zel'dovich *et al.* [13] originally suggested that a detonation can form in a region (''hot spot'') with a suitable gradient of reactivity. The resulting spontaneous reaction wave propagating through that gradient creates a pressure wave that can eventually develop into a shock and then a detonation [14,15]. In confined systems, multidimensional direct numerical simulations (DNS) have shown that hot spots can form through repeated shock-flame interactions and fuel compression by shocks [10].

It remains unclear, however, if and how hot spots could form in unconfined, unpressurized media. The most likely mechanism involves flame interactions with intense turbulence. It was suggested [15,16] that the flame structure could be disrupted by turbulence, producing a distributed flame with reactivity gradients capable of initiating a detonation. There are, however, no realistic *ab initio* experimental or numerical demonstrations of this process. Here we show that high-speed turbulence-flame interactions can indeed lead to DDT, but through a different process in which pressure buildup in the system does not rely on the propagation of global spontaneous reaction waves and, thus, does not require the formation of large-scale gradients of reactivity or distributed flames.

Model and method.—The DNS presented here solve the compressible reactive-flow equations including thermal conduction, molecular species diffusion, and energy release [17,18]. They use an ideal-gas equation of state and a single-step, first-order Arrhenius kinetics to describe chemical reactions converting fuel into product. Simplified reaction-diffusion models represent stoichiometric H_2-air and CH_4-air mixtures with unity Lewis number and reproduce both experimental laminar flame and detonation properties [11]. Simulations were performed with the code ATHENA-RFX, which uses a fully unsplit corner-transport upwind scheme with PPM spatial reconstruction and the HLLC Riemann solver [17–20]. Turbulence is driven using a spectral method [17,21], which ensures that no artificial compressions or rarefactions are introduced in the flow.

Numerical simulations.—Figure 1 shows a traditional combustion regime diagram [22] with a summary of the cases studied. Regions of the diagram representing different burning regimes are bounded by lines of constant nondimensional Damköhler, Da, Karlovitz, Ka, and

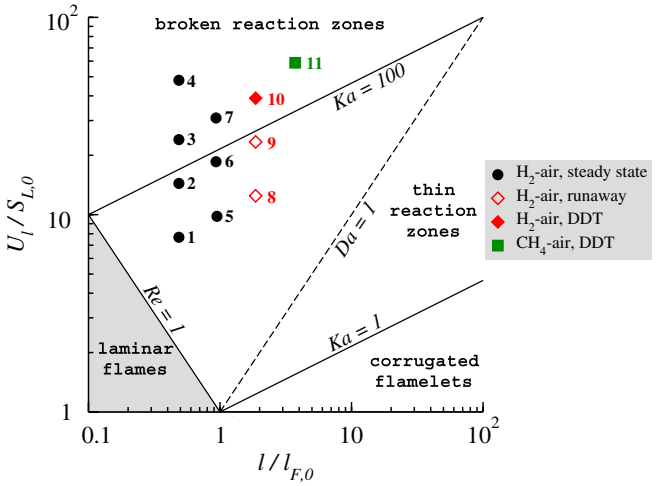

FIG. 1 (color online). Combustion regime diagram [22] showing the simulations discussed here. Symbol color and shape indicate the reactive mixture and the mode of burning. The full flame width $l_{F,0} \approx 2\delta_{L,0}$ [17].

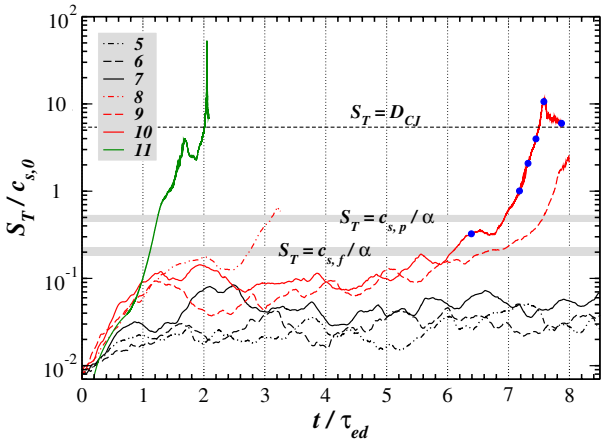

FIG. 2 (color online). The turbulent flame speed, S_T, normalized by the sound speed in cold fuel, $c_{s,0}$. The legend gives the case numbers (Fig. 1). The two shaded gray regions show the range of critical values of S_T [see Eq. (1)] based on the sound speed in fuel, $c_{s,f}$, and product, $c_{s,p}$, for fuel temperatures in the range 360–430 K. Blue dots on the curve for case 10 indicate times of individual profiles in Fig. 3. Time is normalized by the corresponding value of $\tau_{\rm ed}$ in each case.

Reynolds, Re, numbers [22]. Cases 6, 7, and 10 represent several simulations testing numerical issues such as the solution convergence and the absence of unphysical effects due to the boundary conditions. All simulations are well-resolved with the resolution at least $\Delta x = \delta_{L,0}/16$, where $\delta_{L,0}$ cm is the thermal width of the laminar flame in cold fuel [17,18]. Convergence was confirmed for cases 6 [17,18] and 7 using $\Delta x = \delta_{L,0}/8 - \delta_{L,0}/32$, and convergence during the DDT process was confirmed in case 10 for $\Delta x = \delta_{L,0}/8 - \delta_{L,0}/16$.

This Letter focuses on case 10 and later compares it to other simulations shown in Fig. 1. Case 10 is a DNS of a premixed H_2-air flame interacting with the high-speed, steadily driven turbulence. Its setup is similar to the previous detailed study of case 6 [17,18], which analyzed a steady turbulent flame evolution in a smaller system with lower intensity turbulence. The computational domain is a uniform $256 \times 256 \times 4096$ Cartesian mesh with width $L = 0.518$ cm, giving the resolution $\Delta x = \delta_{L,0}/16$ with $\delta_{L,0} \approx 0.032$. Kinetic energy is injected at the scale L to produce homogeneous, isotropic turbulence with the characteristic velocity $U = 1.9 \times 10^4$ cm/s $\approx 63 S_{L,0}$ at the scale L, where $S_{L,0} = 3.02 \times 10^2$ cm/s is the laminar flame speed in cold fuel. The large-scale eddy turnover time is $\tau_{\rm ed} = L/U = 27.3$ μs, the integral velocity is $U_l = 1.2 \times 10^4$ cm/s $\approx 40 S_{L,0}$, and the integral scale is $l = 0.12$ cm. Resulting turbulence away from the flame has an equilibrium Kolmogorov energy spectrum $\propto k^{-5/3}$ in the inertial range extending to scales $\lesssim \delta_{L,0}$ [17].

Initially, fuel has temperature $T_0 = 293$ K and pressure $P_0 = 1.01 \times 10^6$ erg/cm^3. Steady-state turbulence is allowed to develop for $2\tau_{\rm ed}$. At this point ($t = 0$) a planar flame is initialized normal to the x axis. The boundary conditions are zero-order extrapolations at the x boundaries and periodic conditions at the y and z boundaries. After $\approx 2\tau_{\rm ed}$, the turbulent flame is fully developed and reaches a quasi-steady state (QSS) that lasts until $t \approx 6.5\tau_{\rm ed}$. Figure 2 shows the turbulent flame speed, S_T, based on the fuel-consumption rate [17]. Turbulent flame properties during this period are consistent with the earlier analysis of such QSS in case 6 [17,18]. In particular, the flame folded inside the flame brush remains in the thin reaction-zone regime with its reaction-zone structure virtually unaffected by turbulence and its preheat zone broadened by a factor of ≈ 2. S_T is primarily controlled by the increase of the flame surface area with an additional periodic increase $\lesssim 30\%$–40% due to flame collisions and the formation of cusps.

In contrast to case 6, the QSS in case 10 is relatively brief (Fig. 2). After $t \approx 6.5\tau_{\rm ed}$, S_T begins to increase rapidly, becoming supersonic by $7.18\tau_{\rm ed}$ and exceeding the Chapman-Jouguet (CJ) detonation velocity, $D_{\rm CJ}$, at $7.5\tau_{\rm ed}$. DDT occurs at $7.53\tau_{\rm ed}$, and S_T reaches its maximum at $7.58\tau_{\rm ed}$. At $7.63\tau_{\rm ed}$, a fully developed overdriven detonation emerges and quickly relaxes to $D_{\rm CJ}$.

The system evolution during this process is shown in Fig. 3. At $6.39\tau_{\rm ed}$, a slight overpressure arises inside the flame brush, but the energy-generation rate per unit volume, $\dot{E}$, is still close to its value in the planar laminar flame. As the pressure grows and the turbulent flame accelerates, fuel inside the flame brush is compressed and heated. This increases the local flame speed, S_L, causing $\dot{E}$ to rise. At later times, $\dot{E}$ exceeds the laminar value by ~ 2 orders of magnitude. Such accelerated burning leads to further fuel compression and larger S_L. The resulting feedback loop drives a catastrophic runaway process that produces a large pressure buildup and creates strong shocks inside the flame brush. These, in turn, create conditions in which a detonation can arise. (Details of this last stage will be presented in a separate paper.)

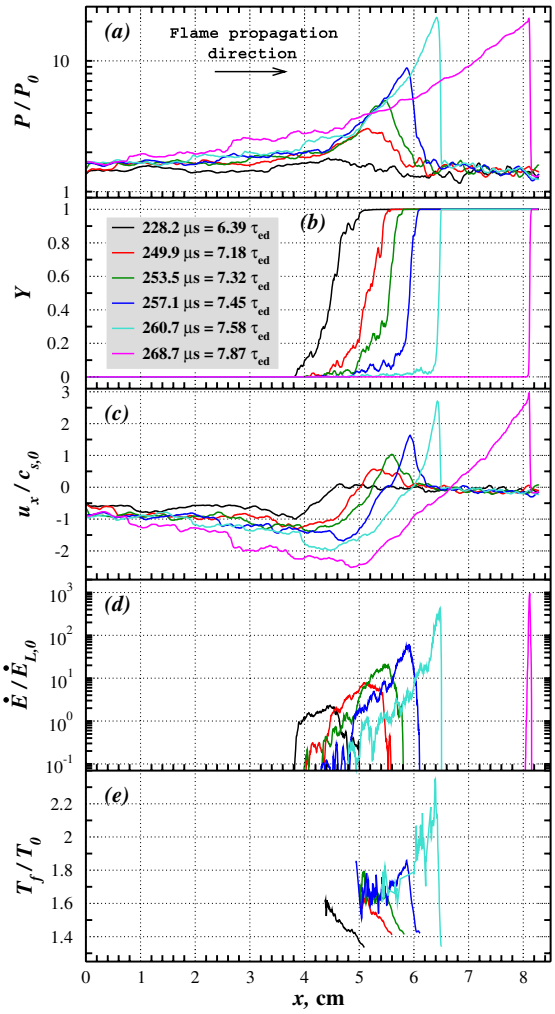

FIG. 3 (color online). The y-z averaged profiles of (a) pressure, P, (b) fuel mass fraction, Y, (c) x velocity, u_x, (d) energy-generation rate per unit volume, $\dot{E}$, and (e) temperature of pure fuel ($Y \geq 0.95$) in case 10. The time from ignition for each profile is shown in panel (b) and indicated with blue dots in Fig. 2. $\dot{E}$ is normalized by its value in a planar laminar flame propagating in cold fuel, $\dot{E}_{L,0} = qS_{L,0}\rho_0/\delta_{L,0}$, where q is the chemical energy release and ρ_0 is the density of cold fuel. T_f is shown inside the flame brush up to the moment of detonation formation ($t \leq 7.58\tau_{\rm ed}$).

Up until the moment of DDT, the average fuel temperature, T_f, inside the flame brush remains <700 K [Fig. 3(e)], and the corresponding induction times are much larger than all dynamical time scales. At all times, the average internal flame structure (reconstructed using method described in [17]) is close to that of a laminar flame in fuel with the corresponding T_f and pressure. Thus, during the runaway, burning is controlled by flame propagation and not by autoignition, which precludes the formation of global spontaneous reaction waves.

Mechanism of the spontaneous runaway.—Consider an unconfined fluid volume V with the total internal energy ε. To increase the pressure inside V (as in Fig. 3), an energetic process must generate energy comparable to ε on the characteristic sound-crossing time of this volume, i.e., $\dot{\varepsilon} \sim \varepsilon/t_s$. If this volume represents a flame with width δ and cross-sectional area L^2, i.e., $V = \delta L^2$, then the burning speed of the flame is defined as $S = \dot{m}/\rho_f L^2$, where $\dot{m} = \dot{\varepsilon}/q$ is the total fuel-consumption rate and ρ_f is the fuel density. Then the condition $\dot{\varepsilon} \sim \varepsilon/t_s$ can be rewritten as $S \sim c_s E/q\rho_f$, where $t_s = \delta/c_s$, c_s is the sound speed, and $E = \varepsilon/V$ is the internal energy per unit volume. The flame here may be laminar, turbulent, or distributed, provided it has the required burning speed.

In order to examine the physical meaning of this condition on S, assume an ideal-gas equation of state, $E = P/(\gamma - 1)$. At the start of the runaway, pressure is nearly constant across the flame. Then the product density is $\rho_p = \rho_f T_f/T_p = \rho_f T_f/(T_f + q/C_p) = P/(P/\rho_f + q(\gamma - 1)/\gamma)$, where T_p is the product temperature and C_p is the specific heat at constant pressure. For energetic reactive mixtures, the denominator $P/\rho_f + q(\gamma - 1)/\gamma$ can be approximated as $q(\gamma - 1)$. In this work, $q = 43.28RT_0/M \gg P_0/\rho_0$ [17] and at the onset of the runaway $P \approx 1.5P_0$ and $\rho_f \approx \rho_0$, giving the accuracy of this approximation $\approx 6\%$. Thus, $\rho_p \approx P/q(\gamma - 1)$, and

$$S \sim \frac{c_s}{q\rho_f} E = \frac{c_s}{\rho_f} \frac{P}{q(\gamma - 1)} \approx \frac{c_s}{\alpha} \equiv S_{\rm CJ}, \qquad (1)$$

where $\alpha = \rho_f/\rho_p$ is the fluid expansion factor.

In the reference frame of a steady flame, $\rho_p U_p = \rho_f U_f = \rho_f S$, where U_f and U_p are the velocities of the fuel and product, respectively. Thus, Eq. (1) is equivalent to the statement that $U_p = c_s$. If c_s is taken as the sound speed in the product, then the flame with the speed satisfying Eq. (1) is a CJ deflagration [23].

The speed of a CJ deflagration, $S_{\rm CJ}$, is a theoretical maximum speed of a steady-state flame. The discussion above shows that such a flame generates enough energy on a sound-crossing time to raise its internal pressure and, thus, disrupt its steady-state structure. Real laminar flames, both chemical [23] and thermonuclear [15], do not have burning speeds that approach $S_{\rm CJ}$. Turbulent flames, however, can develop such high values of S_T.

Unlike a laminar flame, in which the local sound speed increases smoothly from its value in the fuel, $c_{s,f}$, to that in the product, $c_{s,p}$, a turbulent flame effectively consists of two fluids with either $c_{s,f}$ or $c_{s,p}$. Figure 2 shows $S_{\rm CJ}$ based on both $c_{s,f}$ and $c_{s,p}$. Dissipative heating of fuel by turbulence causes $c_{s,f}$ and $c_{s,p}$ to increase and α to decrease. Thus, the horizontal shaded gray areas show the range of values of $S_{\rm CJ}$ corresponding to fuel temperatures $\approx$ 360–430 K. In particular, in case 10, $T_f \approx 360$ K at $2\tau_{\rm ed}$ (lower bound of the shaded regions) and it increases to ≈ 430 K by $6.5\tau_{\rm ed}$ (upper bound).

Figure 2 shows that, upon first reaching the QSS, S_T is close to, but still below, $c_{s,f}/\alpha$, which prevents the onset of the runaway. During the time $(2–6.5)\tau_{\rm ed}$, turbulent heating of fuel increases S_L by a factor of ≈ 2, thus accelerating S_T

above the critical value $c_{s,f}/\alpha$ and allowing the runaway to begin. Figure 3(c) shows that, at this point, the product velocity indeed becomes $\approx c_{s,f}$. Furthermore, the growth rate of S_T increases significantly once S_T becomes $> c_{s,p}/\alpha$, i.e., when U_p becomes supersonic relative to both sound speeds at $t \gtrsim 7\tau_{\mathrm{ed}}$. Note also that the transition from a QSS to a detonation occurs on a sound-crossing time of the turbulent flame $t_s = \delta_T/c_{s,0} \approx 27\ \mu\mathrm{s} \approx \tau_{\mathrm{ed}}$, where $\delta_T \approx 1$ cm is the flame-brush width [Fig. 3(b)] and $c_{s,0} \approx 3.7 \times 10^4$ cm/s.

Figure 2 also shows S_T for turbulent H_2-air flames for other values of U_l and l. In cases 5-7, S_T remains well below $c_{s,f}/\alpha$, and the flame evolves in the QSS, as described in [17,18]. This QSS was observed over significantly longer periods of time than shown in Fig. 2, e.g., $16\tau_{\mathrm{ed}}$ in case 6. Cases 1–4 were similar and so are not shown. The runaway process was also observed in cases 8 and 9, in which, however, the flame accelerated quickly and left the domain before DDT could occur. Note that the overall growth rate of S_T in cases 8 and 9 was lower than in case 10 (τ_{ed} increases with decreasing U_l).

To determine the dependence of the results on the reaction model, we carried out a similar simulation for a stoichiometric CH_4-air mixture. In this case, $\delta_{L,0} = 0.042$ cm is close to that in H_2-air, but $S_{L,0} = 38$ cm/s is 8 times lower [11]. The CH_4-air system also showed DDT, but at a higher turbulent intensity relative to S_L ($U_l = 2.24 \times 10^3$ cm/s $\approx 59 S_L$) and in a larger system ($l = 0.31$ cm, $L = 1.328$ cm) (case 11, Figs. 1 and 2). The overall evolution, however, was different from case 10. The time to DDT was $\approx 2\tau_{\mathrm{ed}}$, and the flame never developed a QSS. The flame accelerated significantly relative to fuel, which required a longer domain to observe DDT, and, in contrast with case 10, a strong well-defined global shock formed and ran ahead of the flame brush.

The key aspect of the spontaneous DDT mechanism discussed here is that it does not place any specific constraints on the equation of state, reaction model, or the flame properties. A decrease of fluid density with increasing temperature in an exothermic process means that, at a high but subsonic burning speed, the flow of products becomes supersonic relative to the flame, irrespective of how burning occurs. This ensures that the pressure wave remains coupled to the region in which the energy release occurs [note the location of peaks of P and $\dot{E}$ in Fig. 3(b) and 3(c)]. This is in contrast with the spontaneous reaction-wave model [13], which requires very specific hot-spot properties in order for the reaction wave and the pressure pulse it produces to remain properly coupled.

Figure 1 suggests that there is both a minimal system size and a minimal relative turbulent intensity at which DDT is possible, and they appear to increase for reactive mixtures with slower laminar flames. Applying Eq. (1) to establish whether DDT can occur depends on our ability to predict the turbulent flame speed for given U_l and l. This is particularly difficult in the high-speed regimes where spontaneous DDT is most likely to occur. Further studies using more detailed chemical kinetics models are required to establish the range of regimes in which DDT is to be expected for realistic reactive mixtures and to investigate the possibility of flame extinction in the presence of high-intensity turbulence.

We thank Vadim Gamezo, Craig Wheeler, and Forman Williams for valuable discussions. This work was supported by the AFOSR grant F1ATA09114G005 and by the ONR/NRL 6.1 Base Program.

*Corresponding author; apol@lcp.nrl.navy.mil

[1] M. A. Nettleton, *Gaseous Detonations* (Chapman and Hall, London, England, 1987).
[2] G. D. Roy, S. M. Frolov, A. A. Borisov, and D. W. Netzer, Prog. Energy Combust. Sci. **30**, 545 (2004).
[3] A. M. Khokhlov, Astron. Astrophys. **245**, 114 (1991).
[4] V. N. Gamezo, A. M. Khokhlov, and E. S. Oran, Phys. Rev. Lett. **92**, 211102 (2004).
[5] A. G. Riess *et al.*, Astron. J. **116**, 1009 (1998).
[6] S. Perlmutter *et al.*, Astrophys. J. **517**, 565 (1999).
[7] E. Mallard and H. L. le Chatelier, Compt. Rend. Acad. Sci. **93**, 145 (1881).
[8] P. Urtiew and A. K. Oppenheim, Proc. R. Soc. A **295**, 13 (1966); M. Kuznetsov, M. Liberman, and I. Matsukov, Combust. Sci. Technol. **182**, 1628 (2010).
[9] L. Kagan and G. Sivashinsky, Combust. Flame **134**, 389 (2003).
[10] E. S. Oran and V. N. Gamezo, Combust. Flame **148**, 4 (2007).
[11] V. N. Gamezo, T. Ogawa, and E. S. Oran, Combust. Flame **155**, 302 (2008); D. A. Kessler, V. N. Gamezo, and E. S. Oran, *ibid.* **157**, 2063 (2010).
[12] V. Bychkov, D. Valiev, and L.-E. Eriksson, Phys. Rev. Lett. **101**, 164501 (2008); M. A. Liberman *et al.*, Acta Astronaut. **67**, 688 (2010).
[13] Ya. B. Zel'dovich, V. B. Librovich, G. M. Makhviladze, and G. I. Sivashinsky, Astronaut. Acta **15**, 313 (1970).
[14] A. K. Kapila, D. W. Schwendeman, J. J. Quirk, and T. Hawa, Combust. Theory Modell. **6**, 553 (2002).
[15] A. M. Khokhlov, E. S. Oran, and J. C. Wheeler, Astrophys. J. **478**, 678 (1997).
[16] J. C. Niemeyer and S. E. Woosley, Astrophys. J. **475**, 740 (1997).
[17] A. Y. Poludnenko and E. S. Oran, Combust. Flame **157**, 995 (2010).
[18] A. Y. Poludnenko and E. S. Oran, Combust. Flame **158**, 301 (2011).
[19] T. A. Gardiner and J. M. Stone, J. Comput. Phys. **227**, 4123 (2008).
[20] J. M. Stone *et al.*, Astrophys. J. Suppl. Ser. **178**, 137 (2008).
[21] M. N. Lemaster and J. M. Stone, Astrophys. J. **691**, 1092 (2009).
[22] N. Peters, *Turbulent Combustion* (Cambridge University Press, Cambridge, England, 2000).
[23] F. Williams, *Combustion Theory* (Perseus Books, Reading, MA, 1985).